

Air Force Institute of Technology

AFIT Scholar

Faculty Publications

3-18-2013

Role of Excited State Photoionization in the 852.1 nm Cs Laser Pumped by Cs-Ar Photoassociation

J. D. Hewitt

University of Illinois at Urbana-Champaign

T. J. Houlahan Jr.

University of Illinois at Urbana-Champaign

Jeffrey E. Gallagher

Air Force Institute of Technology

D. L. Carroll

CU Aerospace

A. D. Palla

CU Aerospace

See next page for additional authors

Follow this and additional works at: <https://scholar.afit.edu/facpub>

 Part of the [Physics Commons](#)

Recommended Citation

J. D. Hewitt, T. J. Houlahan, J. E. Gallagher, D. L. Carroll, A. D. Palla, J. T. Verdeyen, G. P. Perram, J. G. Eden; Role of excited state photoionization in the 852.1 nm Cs laser pumped by Cs-Ar photoassociation. *Appl. Phys. Lett.* 18 March 2013; 102 (11): 111104. <https://doi.org/10.1063/1.4796040>

This Article is brought to you for free and open access by AFIT Scholar. It has been accepted for inclusion in Faculty Publications by an authorized administrator of AFIT Scholar. For more information, please contact richard.mansfield@afit.edu.

Authors

J. D. Hewitt, T. J. Houlahan Jr., Jeffrey E. Gallagher, D. L. Carroll, A. D. Palla, J. T. Verdeyen, Glen P. Perram, and J. G. Eden

RESEARCH ARTICLE | MARCH 18 2013

Role of excited state photoionization in the 852.1 nm Cs laser pumped by Cs-Ar photoassociation

J. D. Hewitt; T. J. Houlahan, Jr.; J. E. Gallagher; D. L. Carroll; A. D. Palla; J. T. Verdeyen; G. P. Perram; J. G. Eden



Appl. Phys. Lett. 102, 111104 (2013)
<https://doi.org/10.1063/1.4796040>

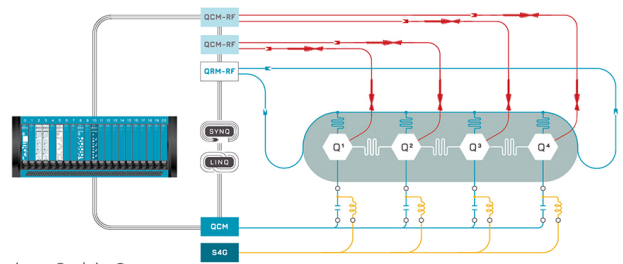


CrossMark



Integrates all
Instrumentation + Software
for Control and Readout of

Superconducting Qubits
NV-Centers
Spin Qubits



Superconducting Qubit Setup

[find out more >](#)

Role of excited state photoionization in the 852.1 nm Cs laser pumped by Cs-Ar photoassociation

J. D. Hewitt,¹ T. J. Houlahan, Jr.,¹ J. E. Gallagher,² D. L. Carroll,³ A. D. Palla,³
 J. T. Verdeyen,³ G. P. Perram,² and J. G. Eden¹

¹Laboratory for Optical Physics and Engineering, Department of Electrical and Computer Engineering, University of Illinois, Urbana, Illinois 61801, USA

²Department of Engineering Physics, U.S. Air Force Institute of Technology, Wright-Patterson Air Force Base, Ohio 45433, USA

³CU Aerospace, Champaign, Illinois 61802, USA

(Received 17 November 2012; accepted 7 March 2013; published online 18 March 2013)

Photoionization of Cs ($6p\ ^2P_{3/2}$) atoms during the operation of a Cs D₂ line (852.1 nm: $6p\ ^2P_{3/2} \rightarrow 6s\ ^2S_{1/2}$) laser, pumped by free→free transitions of thermal Cs-Ar ground state pairs, has been investigated experimentally and computationally. Photoexcitation of Cs vapor/Ar mixtures through the blue satellite of the D₂ transition (peaking at 836.7 nm) selectively populates the $^2P_{3/2}$ upper laser level by the dissociation of the CsAr excited complex. Comparison of laser output energy data, for instantaneous pump powers up to 3 MW, with the predictions of a numerical model sets an upper bound of $8 \times 10^{-26}\ \text{cm}^4\ \text{W}^{-1}$ on the Cs ($6p\ ^2P_{3/2}$) two photon ionization cross-section at 836.7 nm which corresponds to a single photon cross-section of $2.4 \times 10^{-19}\ \text{cm}^2$ for a peak pump intensity of $3\ \text{MW}\ \text{cm}^{-2}$. © 2013 American Institute of Physics. [<http://dx.doi.org/10.1063/1.4796040>]

Lasing on the D₁ lines of Cs and Rb was observed almost a decade ago by photopumping the D₂ transitions ($np\ ^2P_{3/2} \leftarrow ns\ ^2S_{1/2}$, $n = 5$ and 6 for Rb and Cs, respectively) and subsequently relaxing the $n\ ^2P_{3/2}$ state population by $^2P_{3/2} \leftrightarrow ^2P_{1/2}$ fine structure collisional mixing.¹ Proposed and demonstrated in Rb in 2003 by Krupke *et al.*,² this classical three-level laser is characterized by exceptional quantum efficiencies¹⁻³ and has proven to be an efficient mode converter for diode laser arrays, as evidenced by the recent report⁴ of a diode bar-pumped Cs 894 nm laser generating a maximum output power of $\sim 1\ \text{kW}$ with a pump conversion efficiency of 48%. Owing to the modest ionization potentials of the alkali atoms (3.9 eV for Cs), photoionization of the $n\ ^2P_{1/2}$ upper laser level is of potential concern⁵ as one mechanism for removing neutral atoms from the pump/lase cycle.

In this letter, the results of experiments and simulations designed to investigate the photoionization of Cs ($6p\ ^2P_{3/2}$) in an optically pumped Cs laser operating at 852.1 nm are described. Excitation of the blue satellite associated with the Cs D₂ transition in Cs-Ar mixtures^{6,7} with laser pulses having intensities adjustable up to $3\ \text{MW}\ \text{cm}^{-2}$ demonstrate that photoionization plays a minor role in the dynamics of the laser. Optical pumping of Cs-Ar pairs to the dissociative $B^2\Sigma_{1/2}^+$ state of the alkali-rare gas diatomic complex, correlated with $\text{Cs}(6p\ ^2P_{3/2}) + \text{Ar}(^1S_0)$ in the separated atom limit, populates the 852.1 nm laser upper level selectively and with a quantum efficiency above 98%. Known as an XPAL laser system, this pump/lase cycle for thermal alkali-rare gas pairs has two distinct assets insofar as photoionization losses are concerned: (1) the spectral brightness of the pump can be reduced by 1–2 orders of magnitude relative to the classical three level atomic system (Refs. 2 and 3) and (2) the breadth of the laser excitation spectrum allows for the pump wavelength to be set so as to maximize the detuning of the pump

photon energy from an alkali excited state resonance. Avoiding or minimizing resonantly enhanced, two photon ionization processes constrains the overall photoionization loss rate. For the present experiments, comparison of laser output data with numerical simulations indicates that an upper bound on the cross-section for two photon ionization of Cs ($6p\ ^2P_{3/2}$) at 836.7 nm is $8 \times 10^{-26}\ \text{cm}^4\ \text{W}^{-1}$ which corresponds to a single photon cross-section of $2.4 \times 10^{-19}\ \text{cm}^2$ for a peak pump intensity of $3\ \text{MW}\ \text{cm}^{-2}$. Predictions of the numerical model reproduce experimental results over a range in Cs number density of almost two orders of magnitude.

Figure 1 is a schematic diagram of the experimental arrangement which is similar to that employed previously.^{6,7} A pulsed dye laser, operating at a repetition frequency of 10 Hz and pumped by a frequency-doubled, Nd-doped yttrium aluminum garnet (Nd:YAG) laser, serves as the optical pump for these experiments. A solution of the laser dye LDS-821 in propylene carbonate provided pulse energies at 836.7 nm (when in an oscillator/two stage amplifier system) adjustable from $\sim 3.5\ \text{mJ}$ to more than 35 mJ. Owing to the laser geometry and the saturation intensity for the dye/solvent medium itself, the diameter of the dye laser output beam increases monotonically with pulse energy from $\sim 5\ \text{mm}$ to 11 mm (FWHM). This variation was characterized in detail in an effort to maximize the accuracy of the model. Raising the pump pulse energy over the interval noted earlier was also accompanied by an increase in the dye laser temporal width from 6 to 11 ns (FWHM). Pump laser pulses entered the optical cavity, comprising two 3 m radius of curvature mirrors separated by 52 cm, by means of a polarizing beam splitter. The reflectivities of the high reflector and output coupler at 852 nm were $>99\%$ and 50%, respectively. No effort was made to optimize the cavity output coupling. A mixture of natural abundance Cs and 500 Torr of Ar

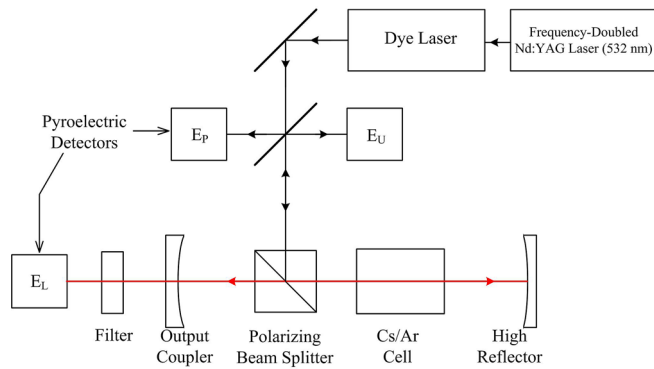


FIG. 1. Schematic diagram of the experimental arrangement. Dye laser pulse energies were variable from ~ 3.5 mJ to more than 35 mJ. The length of the Cs/Ar cell was 10 cm and the Ar number density was fixed at $[\text{Ar}] = 1.6 \times 10^{19} \text{ cm}^{-3}$ throughout the experiments. Mirror reflectivities at 852 nm were $>99\%$ for the high reflector and 50% for the output coupler.

(300 K) was contained within a borosilicate cell having a length, diameter, and clear aperture of 10 cm, 2.5 cm, and 2.1 cm, respectively. Residual pump radiation exiting the cavity through the output coupler was blocked by an 852.1 nm interference filter, and three calibrated pyroelectric detectors monitored the pulse energies associated with the Cs laser (E_L), the unabsorbed pump (E_U), and the incoming dye laser beam (E_P).

Data representative of those obtained in the present experiments are illustrated in Fig. 2. Measurements of the variation of the laser output pulse energy E_L with the absorbed pump energy E_A are presented for six Cs/Ar cell temperatures in the 433–534 K interval, which corresponds to Cs number densities from $3.5 \times 10^{14} \text{ cm}^{-3}$ to $1.4 \times 10^{16} \text{ cm}^{-3}$. Throughout these measurements, the excitation wavelength (λ_p) was fixed at 836.7 nm which coincides with the peak of the Cs D_2 line blue satellite in Cs-Ar mixtures. Virtually all of the data exhibit an abrupt shift in functional form at low 852.1 nm intensities and the inset to Fig. 2 displays this behavior clearly for the $T = 474$ K data

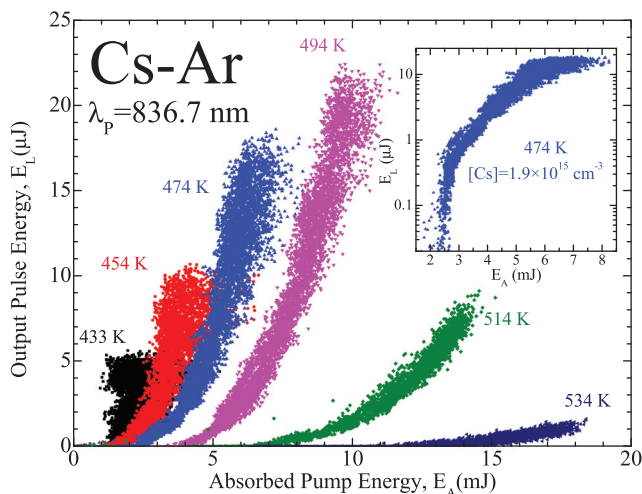


FIG. 2. Dependence of the Cs 852.1 nm laser output energy (E_L) on the absorbed pump pulse energy (E_A) when the pump wavelength λ_p is fixed at 836.7 nm. Data are given for measured Cs/Ar cell temperatures in the 433–534 K interval which corresponds to Cs densities ranging from $3.5 \times 10^{14} \text{ cm}^{-3}$ to $1.4 \times 10^{16} \text{ cm}^{-3}$. The inset shows the $T = 474$ K data in semilog format.

plotted in a semilog format. We attribute the obvious transition observed at $E_L \approx 0.4 \mu\text{J}$ to the onset of saturation of the laser because the intracavity intensity at this point ($50\text{--}100 \text{ W cm}^{-2}$) is larger than, but consistent with, estimates of the Cs D_2 line saturation intensity $I_{\text{sat}} \sim 10 \text{ W cm}^{-2}$. For absorbed pump pulse energies E_A beyond 2–3 mJ, the output power rolls over as the laser exhibits the behavior of a conventional saturated amplifier. In this regard, it must be remembered that the effective length of the amplifier grows with increasing E_A because the corresponding rise in pump pulse width accommodates ~ 6 passes through the gain medium at high pulse energies ($E_A \geq 12$ mJ), whereas only ~ 3 passes are available at the lowest pump intensities. It should also be mentioned that the increase in threshold pump power that accompanies rising temperature (i.e., Cs number density) is consistent with the ground state depletion required to obtain a population inversion on the D_2 line which is a resonance transition.

In order to rigorously evaluate the experimental data, the BLAZE V model described by Palla *et al.*⁸ was adopted and modified. Originally developed to analyze Cs lasers pumped by the photoassociation of thermal alkali rare-gas atoms, this model has been modified in several respects for the present work. Because (as noted earlier) the pump beam cross-sectional area changed as the energy was increased, this effect was accounted for explicitly in the model. Specifically, the variation of the spatial extent of the pump beam is accurately described by the relation: $d = A + B \log(E_P)$, where A and B are constants, E_P is expressed in mJ, and d is the beam diameter (FWHM). For example, the value of d for $E_P = 3.5$ mJ is 5 mm, while that for 35 mJ is 11 mm. Although the temporal width of the pump pulse also increased, from 6 to 11 ns, as the pump pulse energy was raised, the influence of this parameter on the simulation results is weak and the nominal value of 8 ns (FWHM) was adopted for the discussion to follow. An unanticipated benefit of a detailed comparison of experiment with the model over a broad range in temperature is that the computational predictions identified a systematic error in the experimental measurements of cell temperature. The design of the optical cell and oven was such that reliable measurements of the Cs vapor pressure could be made for $T \leq 450$ K. At higher temperatures, however, a small but significant difference (δT) was found to exist between the experimental and predicted temperature values which does not appear to be attributable to the growing influence of Cs dimer (Cs_2) formation⁹ or to other factors. Rather, the discrepancy is likely the result of the apparatus itself and the experimental procedure. The temperatures given in Fig. 2 are the experimental values (T_{exp}), and $\delta T (\equiv T_{\text{exp}} - T_{\text{model}})$ is found to rise from zero at $T_{\text{exp}} = 454$ K to 24 K when T_{exp} is 534 K.

In these experiments, the instantaneous pump power reaches values above 3 MW which is considerably higher than those of previous studies.^{6,7} Accordingly, the incorporation of excited state photoionization into the simulations is essential and we first consider the dominant pathway(s) for this loss mechanism. The absorption of a single photon by the $6p \ ^2P_{3/2}$ state is not a favorable route because the detuning Δ , relative to the $8s \ ^2S_{1/2} \leftarrow 6p \ ^2P_{3/2}$ and $6d \ ^2D_{5/2} \leftarrow 6p \ ^2P_{3/2}$ resonances, is $\sim 636 \text{ cm}^{-1}$ (19 THz) and 1050 cm^{-1} (31 THz),

respectively, for a $\lambda = 836.7$ nm photon. Assuming the coefficient for pressure broadening of the $6d \leftarrow 6p$ and $8s \leftarrow 6p$ lines in Cs to be no more than a factor of 4 larger than that for the $6p \ ^2P_{3/2} \leftarrow 6s$ transition,¹⁰ then the linewidth (FWHM) of both transitions when broadened by Ar at a number density of $1.6 \times 10^{19} \text{ cm}^{-3}$ is $< 0.5 \text{ cm}^{-1}$. If the functional form for the far-wing of the alkali absorption profiles is taken to be a Lorentzian, one finds that the absorption cross-section 636 cm^{-1} into the blue tail (i.e., the terminus of an 836.7 nm photon) of the $8s \ ^2S_{1/2} \leftarrow 6p \ ^2P_{3/2}$ lineshape, for example, is suppressed by more than six orders of magnitude relative to its peak value. Because the detuning from the $6d \ ^2D_{5/2} \leftarrow 6p \ ^2P_{3/2}$ transition is almost double that for the $8s \leftarrow 6p$ lines, we deem the $6p \ ^2P_{3/2}$ photoionization rates associated with the sequential absorption of two pump photons to be negligible, and we estimate non-resonant two-photon ionization to be dominant. It should be mentioned, however, that, at the rare gas pressures characteristic of these experiments, optical transitions between alkali-rare gas diatomic molecular states are undoubtedly influential with regard to the photophysics of the upper laser level. Consequently, detailed laser spectroscopic studies of the Cs-Ar interaction potentials correlated with Cs ($6p$, $6d$, $8s$) + Ar in the separated atom limit will ultimately be necessary to confirm or contradict the presumption that neglects photoionization of Cs($6p \ ^2P_{3/2}$) by the sequential absorption of two photons.

Accordingly, the nonlinear process: $\text{Cs} (6p \ ^2P_{3/2}) + 2\hbar\omega \xrightarrow{\sigma^{(2)}} \text{Cs}^+(^1S_0) + e^- + \Delta E$, where $\sigma^{(2)}$ is the two-photon ionization cross-section expressed in $\text{cm}^4 \text{ W}^{-1}$ and ΔE is the energy beyond that required for two 836.7 nm photons, was incorporated into the model. In Fig. 3, the predictions of the numerical simulations for $\sigma^{(2)} \leq 10^{-27} \text{ cm}^4 \text{ W}^{-1}$ are superimposed onto the data of Fig. 2. The lower temperature of the two indicated for several data sets is the temperature assumed by the model. Despite the underestimate of the pump energy threshold for the 434 K data, the model and experiment are in agreement when the two photon ionization cross section lies at or below this limit. Not only are the model predictions of Fig. 3 insensitive to variations of a factor of two or more in the assumed values for cross-sections and lifetimes but one asset of simulations involving low-lying states of the atomic alkalis is that

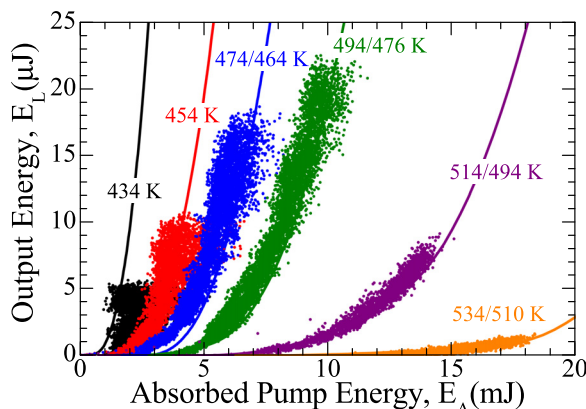


FIG. 3. Comparison of the data of Fig. 2 with model predictions when $\sigma^{(2)} \leq 10^{-27} \text{ cm}^4 \text{ W}^{-1}$. All temperatures indicated are experimental (cell wall) values.

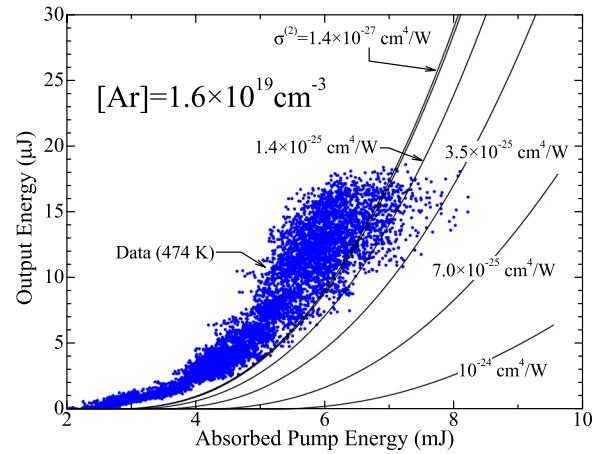


FIG. 4. Experimental data obtained at 474 K, as compared to the numerical simulation predictions for $T = 464 \text{ K}$ and six values of $\sigma^{(2)}$ between $1.4 \times 10^{-27} \text{ cm}^4 \text{ W}^{-1}$ and $1 \times 10^{-24} \text{ cm}^4 \text{ W}^{-1}$.

the constants required by the model are generally well-known. A more detailed comparison of the predictions of the simulations with experimental results is given in Fig. 4 for the $T = 474 \text{ K}$ ($[\text{Cs}] = 1.9 \times 10^{15} \text{ cm}^{-3}$) data. The solid curves represent model predictions for $T = 464 \text{ K}$ and $\sigma^{(2)}$ varied between $1.4 \times 10^{-27} \text{ cm}^4 \text{ W}^{-1}$ and $1 \times 10^{-24} \text{ cm}^4 \text{ W}^{-1}$. When $\sigma^{(2)} \leq 10^{-25} \text{ cm}^4 \text{ W}^{-1}$, the simulations describe the experiments well, whereas $\sigma^{(2)}$ values above $3.5 \times 10^{-25} \text{ cm}^4 \text{ W}^{-1}$ yield predicted laser output energies that clearly deviate from the data. A similar conclusion is reached for all six data sets ($434 \leq T \leq 534 \text{ K}$) and Fig. 5 provides a second example for the $T = 514 \text{ K}$ experiments. In this case, the model predictions for both $\sigma^{(2)} = 1.4 \times 10^{-27} \text{ cm}^4 \text{ W}^{-1}$ and $1.4 \times 10^{-26} \text{ cm}^4 \text{ W}^{-1}$ match the data well but a significant discrepancy between experiment and the calculations is evident for $\sigma^{(2)} = 1.4 \times 10^{-25} \text{ cm}^4 \text{ W}^{-1}$.

Examination of results similar to those of Figs. 4 and 5 indicate that $\sigma^{(2)}$ is no larger than $8 \times 10^{-26} \text{ cm}^4 \text{ W}^{-1}$, a value corresponding to a single photon ionization cross-section of $2.4 \times 10^{-19} \text{ cm}^2$ when the 836.7 nm optical field intensity is 3 MW cm^{-2} . At this intensity, the Cs $6p \ ^2P_{3/2}$ two photon ionization loss rate is $3 \times 10^6 \text{ s}^{-1}$. We note that, for the intensity specified in Ref. 5 for a Cs XPAL laser (500 kW cm^{-2}), the loss rate is $8 \times 10^4 \text{ s}^{-1}$ which is 1.5 orders of magnitude

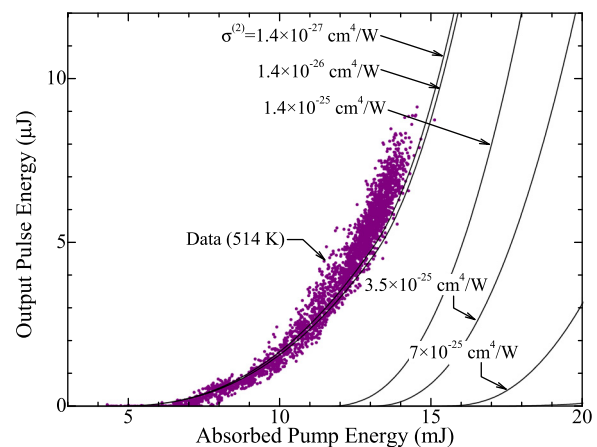


FIG. 5. Comparison of the $T = 514 \text{ K}$ data with model predictions for $T = 494 \text{ K}$ and $1.4 \times 10^{-27} \leq \sigma^{(2)} \leq 7 \times 10^{-25} \text{ cm}^4 \text{ W}^{-1}$.

smaller than that calculated by Knize *et al.*⁵ One potential source of this discrepancy is the adoption in Ref. 5 of a single photon process to describe the photoionization of the alkali atomic $n^2P_{1/2,3/2}$ states ($n = 6$ for Cs) by laser emission at the wavelengths of the D₁ or D₂ lines. However, the photoionization of any alkali atom (in its lowest excited state(s)) by D₁ or D₂ transition radiation requires the absorption of at least two photons. In addition, the cross-section for the single photon ionization process was assumed⁵ to be 2×10^{-17} cm². Although few data are available in the literature with which the present results (or those of Ref. 5) can be compared, we note that Nayfeh *et al.*¹¹ estimated the single photon cross-section for the ionization of the Cs (7p) states at $\lambda = 455$ nm to be 3×10^{-18} cm² or approximately one order of magnitude smaller than the photoionization cross-section of Ref. 5.

In summary, experimental measurements of the output energy of the Cs D₂ line (852.1 nm) laser, pumped at 836.7 nm in Cs-Ar mixtures, have been analyzed with a numerical model that incorporates two photon ionization of the upper laser level. Comparison of model predictions with experimental data over a range in Cs number density of almost two orders of magnitude demonstrates that the upper bound on the cross-section for two photon ionization of the Cs ($6p\ ^2P_{3/2}$) state is 8×10^{-26} cm⁴ W⁻¹. This cross-section is to be expected for excited state photoionization of a “one electron” atom having a Xe core but stands in contrast to the cross-section measured for two photon ionization of Xe at 193 nm ($\sigma^{(2)} = 4 \times 10^{-32}$ cm⁴ W⁻¹),¹² a process in which a 5p electron is removed from the closed-shell ground state configuration of the Xe atom. The specific photoionization measurements reported here, in which the pump wavelength

does not coincide with either the Cs D₁ or D₂ lines, suggest that photoionization losses are not likely to be of concern for high power, CW XPAL lasers.

The support of this work by the U.S. Air Force Office of Scientific Research (AFOSR) and the High Energy Laser Joint Technology Office (HEL-JTO) under Grant Nos. FA9550-10-1-0048 and FA9550-07-1-0575, respectively, is gratefully acknowledged.

¹W. F. Krupke, *Prog. Quantum Electron.* **36**, 4 (2012).

²W. F. Krupke, R. J. Beach, V. K. Kanz, and S. A. Payne, *Opt. Lett.* **28**, 2336 (2003).

³R. J. Beach, W. F. Krupke, V. K. Kanz, S. A. Payne, M. A. Dubinskii, and L. D. Merkle, *J. Opt. Soc. Am. B* **21**, 2151 (2004).

⁴A. V. Bogachev, S. G. Garanin, A. M. Dudov, V. A. Yeroshenko, S. M. Kulikov, G. T. Mikaelian, V. A. Panarin, V. O. Pautov, A. V. Rus, and S. A. Sukharev, *Quantum Electron.* **42**, 95 (2012) [*Kvantovaya Elektron. (Moscow)* **42**, 95 (2012)].

⁵R. J. Knize, B. V. Zhdanov, and M. K. Shaffer, *Opt. Express* **19**, 7894 (2011).

⁶J. D. Readle, C. J. Wagner, J. T. Verdeyen, T. M. Spinka, D. L. Carroll, and J. G. Eden, *Appl. Phys. Lett.* **94**, 251112 (2009).

⁷J. D. Readle, J. G. Eden, J. T. Verdeyen, and D. L. Carroll, *Appl. Phys. Lett.* **97**, 021104 (2010).

⁸A. D. Palla, D. L. Carroll, J. T. Verdeyen, and M. C. Heaven, *J. Phys. B* **44**, 135402 (2011).

⁹M. Lapp and L. P. Harris, *J. Quant. Spectrosc. Radiat. Transf.* **6**, 169 (1966).

¹⁰W. Demtröder, *Laser Spectroscopy*, 3rd ed. (Springer-Verlag, Berlin, 2003).

¹¹M. H. Nayfeh, G. S. Hurst, M. G. Payne, and J. P. Young, *Phys. Rev. Lett.* **39**, 604 (1977); **41**, 302 (1978).

¹²A. W. McCown, M. N. Ediger, and J. G. Eden, *Phys. Rev. A* **26**, 3318 (1982).